water

MDPI

Article

Long-Term Trend and Variability of Volume Transport and Advective Heat Flux through the Boundaries of the Java Sea Based on a Global Ocean Circulation Model (1950–2013)

Rima Rachmayani, Nining Sari Ningsih *, Farrah Hanifah and Yasmin Nabilla

Research Group of Oceanography, Faculty of Earth Sciences and Technology, Institut Teknologi Bandung, Jl. Ganesa No. 10, Bandung 40132, Indonesia
* Correspondence: nsningsih@itb.ac.id

Abstract: The variability and trend of volume and advective heat flux, in addition to the net inflow and outflow of advective heat flux in the Java Sea for 64 years (1950–2013), along with its relationship with the monsoon, ENSO (El Niño Southern Oscillation), and IOD (Indian Ocean Dipole), have all been studied. A simulation of the 3D hydrodynamic HYCOM (HYbrid Coordinate Ocean Model) with a 1/8° grid resolution was performed in this study. Judging from the simulated results, the seasonal variability, which has a period of 12 months, has a very significant impact on contributing to the variability and trend of volume and advective heat flux, as well as the net inflow and outflow of advective heat flux in the Java Sea for 64 years. This is followed by interannual variability, which has a time range of 1.5–6.5 years, and interdecadal variability, with a period of 21.3–32 years. The interannual variability in the Java Sea is strongly caused by ENSO and IOD. El Niño and a positive IOD caused a weakening of southward transport through Karimata and the Bangka Strait. On the contrary, southward transport strengthened during La Niña and the negative IOD. Furthermore, La Niña and a positive IOD both strengthen (weaken) the transport westward (eastward) in the Sunda Strait (Eastern Java). On the other hand, El Niño and a negative IOD weaken (strengthen) the westward (eastward) transport in the Sunda Strait (Eastern Java). According to the findings, the IOD effect is stronger than the ENSO effect in the Java Sea. The inflow and outflow of volume transport in the Java Sea are in balance, but not the advective heat flux. The advective heat transported through Karimata and Bangka Strait to the Java Sea is up to 0.216 PW, while the total advective heat flux through the outflow straits (Sunda Strait and Eastern Java) is 0.220 PW. Thus, the net advective heat flux out of the Java Sea is 0.004 PW, allegedly obtained from an atmosphere–sea interaction in which the sea received heat from the atmosphere.

Keywords: volume; heat; transport; ENSO; IOD; Java Sea

check for updates

Citation: Rachmayani, R.; Ningsih, N.S.; Hanifah, F.; Nabilla, Y. Long-Term Trend and Variability of Volume Transport and Advective Heat Flux through the Boundaries of the Java Sea Based on a Global Ocean Circulation Model (1950–2013). *Water* **2023**, *15*, 740. https://doi.org/10.3390/w15040740

Academic Editor: Changming Dong

Received: 24 December 2022
Revised: 30 January 2023
Accepted: 5 February 2023
Published: 13 February 2023

1. Introduction

The Indonesian Throughflow (ITF) is significant for the global climate system and acts as the top branch of the global heat conveyor belt [1]. The total mass of water transported through a cross-sectional area is defined as “transport volume”, and it is heavily influenced by the current. Similarly, advective heat flux occurs at sea in addition to volume transport and is influenced by currents, temperature, and water density [2,3]. Therefore, understanding the variability of advective heat flux is critical to understanding climate change [4,5]. A western route through the South China Sea (SCS), the Karimata Strait, and the Java Sea are one of the main ITF input paths [6,7]. Because of its lower water depths, it was formerly believed that the ITF intake through the western route had no impact on the main ITF [8–11]. Recent research has shown that the primary ITF’s seasonal magnitude and variability are significantly influenced by the SCS-Indonesian Seas transport/exchange (SITE) through the Karimata Strait, mostly as a result of the alternating monsoon forcing [12–21]. According to [5], advective heat flux is dominant in the Atlantic and Pacific Oceans, while strong advective heat flux exists between the Pacific and Indian Oceans. Research in [4] conducted an analysis in the SCS on volume transport, advective heat flux, and net heat flux with smaller coverage and higher resolution. Investigation of the importance of the upper ocean zonal and meridional volume transport in the Arabian Sea and the Bay of Bengal simulated with a higher resolution of regional modeling Massachusetts Institute of Technology General Circulation Model (MITgcm) of ~10 km horizontal resolution, in order to realistically simulate circulation and hydrography in the area is conducted by [22]. In the identical domain and configuration of MITgcm, [23] carried out several sensitivity experiments to understand and quantify the role of air–sea forcing on the surface and sub-surface hydrography, circulation, and mixed layer depth.

A study of [4] discovered that the advective heat flux that exits the SCS was 0.059 PW greater than that enters the SCS. This excess heat is thought to be caused by the ocean-atmosphere interaction, in which the atmosphere provides a heat input of 0.059 PW to the SCS [24]. Numerous recent studies have revealed that the SCS has a substantial influence on the ITF [13–15,17,25–27] and is crucial to Southeast Asia's climate system [28,29]. The heat and freshwater budgets associated with the SCS interoceanic circulation (Luzon, Taiwan, Mindoro, Balabac, Karimata, and Malacca) are well recognized [4,11,19]. This study will discuss volume transport, advective heat flux, and net advective flux in and out of the Java Sea, similar to what [4] did in the SCS. A study [30] investigated volume transport in Indonesian waters and discovered that the Java Sea's mean volume transport enters through the Karimata Strait and exits through the Sunda Strait and East Java. Research in [31] investigated the variability of volume transport in the Karimata Strait, the Sunda Strait, and East Java and concluded that monsoons, ENSO (El Niño Southern Oscillation), and the Dipole Mode (DM) event all have a strong influence on circulation in these three straits [32,33]. Farther to the west in the Indian Ocean, [34] attempted to inspect the main large-scale patterns of intra-seasonal mixed layer depth (MLD) variations and assess their potential impact on the related sea surface temperature (SST) response. Using oceanic simulation, the active or break phase of the Indian monsoon in summer and the Madden-Julian Oscillation (MJO) in winter are the drivers of MLD variations in the Indian Ocean. Moreover, [35] investigated that the Indian Ocean Dipole (IOD) is responsible for most variations in the 10° N–10° S-band, with positive phases associated with a shallow MLD in the equatorial and south-eastern Indian Ocean and a deepening in the south-central Indian Ocean.

In the case of the Java Sea, even with its interoceanic passageways, the Java Sea has not yet been thoroughly investigated in terms of both observations and numerical models [36–38]; in particular, the importance of the variability and trend of volume and advective heat flux, in addition to the net inflow and outflow of advective heat flux that supports the ecosystems in the Java Sea, such as fish and seagrass ecosystems. The inflow and outflow of advective heat flux and volume transport in the Java Sea, as well as the net advective heat flux in these waters, are calculated and analyzed in this study. Although seasonal variability will be explained, the discussion will focus on interannual and decadal variability due to the length of the data used from 1950 to 2013 (64 years). The volume transport and advective heat flux trends (linear trend) in the Java Sea straits will also be observed. The goal of this study is to investigate the volume transport and advective heat flux characteristics, as well as calculate the net advective heat flux in and out of the Java Sea over a 64-year period using a three-dimensional (3D) hydrodynamic model of HYbrid Coordinate Ocean Model (HYCOM) with a 1/8° grid resolution. Thus, the long-term trend and variability of advective heat flux and volume transport in the Java Sea's interoceanic channels (Java Sea) are investigated.

In order to determine the existence of net heat gain across the surface of the Java Sea, it is necessary to analyze the Java Sea interoceanic circulation and its related heat budget [29,39–41]. To understand the long-term trend and variability of volume transport and advective heat flux through the Java Sea's boundaries, Section 2 discusses the significance of data and model simulation. The study's results are presented in Section 3.

In comparison to other earlier research, Section 4 presents a thorough investigation of the long-term trend and variability of volume transport and advective heat flux, and the conclusion is summarized in Section 5.

2. Materials and Methods

Figure 2.1a shows the Indonesian waters from the global model, which includes the Java Sea boundaries and a regional area of interest at 21.5° S–23° N and 90°–139° E. (Figure 2.1b). As shown in Figure 2, four transects—Karimata Strait (transect 1), Bangka Strait (transect 2), Sunda Strait (transect 3), and Eastern Boundary of Java Sea (transect 4)—have been chosen as paths for volume transport and advective heat flux in the Java Sea.

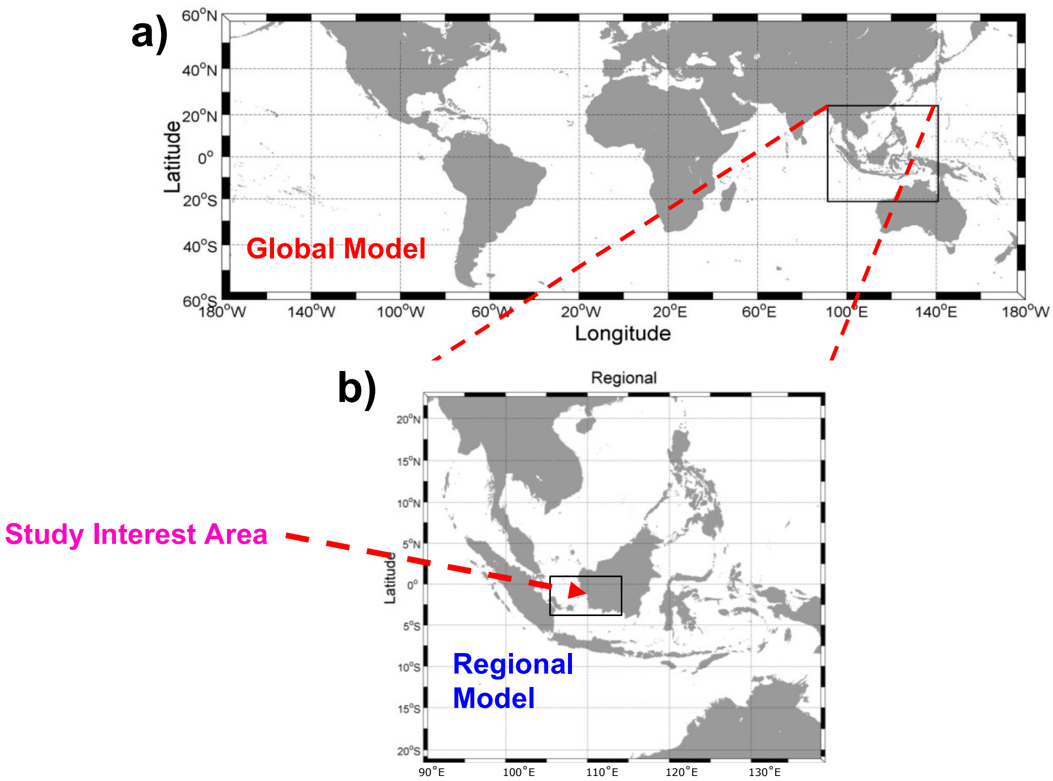

Figure 1. Indonesian maritime domain drawn from the global model (**a**), and Java Sea boundaries taken from the regional model (**b**).

2.1. Data

The Java Sea's features, volume transport variability, and advective heat flux were studied using bathymetry, monthly density, temperature, and ocean current data from the HYCOM. Table 1 summarizes the data information for model input and verification. In order to examine the interannual variability in volume transport as well as advective heat flux, supporting data from the Ocean Niño Index (ONI) and Dipole Mode Index (DMI) were taken into consideration. The National Oceanic and Atmospheric Administration (NOAA) and Japan Agency for Marine-Earth Science and Technology (JAMSTEC) provided the data, which were acquired from their respective websites. To examine the decadal variability, Pacific Decadal Oscillation (PDO) data from the Joint Institute for the Study of Atmosphere and Ocean (JISAO) (http://research.jisao.washington.edu (accessed on 12 May 2015)) were used. Additionally, the transport trend into and out of the Java Sea was examined using wind data from the National Centers for Environmental Prediction (NCEP).

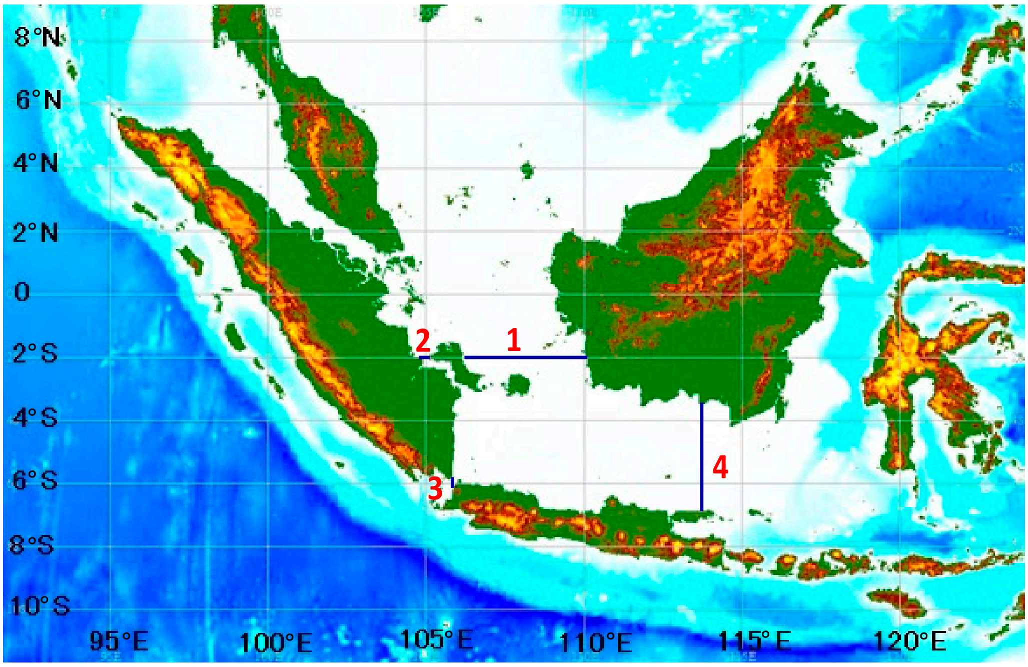

Figure 2. The Java Sea with four dark blue-lined transects: (1) Karimata Strait, (2) Bangka Strait, (3) Sunda Strait, (4) Eastern Boundary of Java Sea (EBoJS) (Modified after [42]).

Table 1. Information about data used for model input and verification.

	Parameter	Resolution	Period	Source	References
Model Input	Bathymetry	$2'$	-	ETOPO2	[43]
	Temperature	-	-	LEVITUS94	[44–47]
	Salinity				
	Air Temperature	1875°	1949–2013	NCEP Reanalysis	[48]
	Humidity				
	Rainfall				
	Solar Radiation				
	Wind				
	SST (assimilation)	1875°	1949–2013	NCEP Reanalysis	[48]
Verification	Surface Current	1°	1993–2013	Ocean Surface Current Analyses (OSCAR)	[49,50]
	SSHA	1/3°	1993–2010	AVISO	
	SST	2°	1949–2013	NOAA	

2.2. Model Setup Experiment

In this study, the HYCOM was simulated in three dimensions [51]. Two alternative spatial resolution scenarios—a global model with a grid resolution of 1/2° and a regional model with a grid resolution of 1/8°—were utilized to conduct the simulations (Figure 2.1). Three steps of the simulation are performed as follows: (1) spin-up simulation for 20 years, (2) simulate the global model, and (3) run the regional model for each 64-year period between 1950 and 2013 [50,52]. In addition, the verification of the HYCOM simulation performed in this study is documented in [52]. Table 2 provides details on the global and regional models.

Table 2. Setting of the experiment for global and regional models.

	Global Model	Regional Model
Model Domain	60° S–60° N and 180° W–180 VE	21.5° S–23° N and 90° E–139° E
Resolution	1/2°	1/8°
Layer	22	22
Bathymetry	ETOPO2 (2′ resolution)	ETOPO2 (2′ resolution) + DISHIDROS map
Simulation Period	64 years (1950–2013)	64 years (1950–2013)

3. Results

3.1. Zonal and Meridional Volume Transport and Advective Heat Flux through the Boundaries of the Java Sea

Volume transport and advective heat flux calculations in the Sunda Strait, East Java, and Karimata Strait have been done in a number of studies. Tables 3 and 4 provide a comparison of the volume transport and advective heat flux calculations used in this investigation with those used in earlier studies, respectively. In this study, movement to the north or east is indicated by a positive value for transport, whereas movement to the south or west is shown by a negative number. Transport with negative signs is obtained from all studies' calculations of the volume transport and advective heat flux (−1.97 and −0.204) in the Karimata Strait, suggesting that the volume transport and advective heat flux have migrated into the Java Sea. However, the amount of transport calculated for each investigation varies. This could be caused by differences in the computation strategy, the number of grids, or other factors. For example, along with the Karimata Strait, the mean of volume transport (advective heat flux) conveyance into the Java Sea by the Bangka Strait is −0.12 PW (−0.012 PW), whereas volume transport (advective heat flux) exits of the Java Sea is provided by the Sunda Strait and Eastern boundary of Java Sea (EBoJS) at (−0.70 PW) −0.072 PW and (1.39) 0.148 PW, respectively (Tables 3 and 4).

Table 3. Volume transport in Karimata Strait, Bangka Strait, Sunda Strait, and Eastern Boundary of the Java Sea are compared to earlier research. Positive (negative) values indicate north or east (south or west) transport.

Source	Volume Transports (Sv = 10^6 m^3/s)				Period of Data	Method
	Karimata Strait (1)	Bangka Strait (2)	Sunda Strait (3)	Eastern Boundary of the Java Sea (4)		
[53]			−0.30		1992–2000 (9 years)	Numerical Model (OCCAM, 1/4°)
[26]	−2.10					Numerical Model
[31]	−1.01		−0.62	0.29	1959–2002 (44 years)	Numerical Model (HAMSOM, 1/6°)
[13]	−1.30					Numerical Model
[4]	−1.16				1982–2003 (22 years)	Numerical Model (1/6°)
[54]	−0.30					Numerical Model
[18]	−1.60					Numerical Model
[19]	−0.80				December 2007–November 2008 (1 year)	Roughly estimate from ADCP measurement
[21]	−0.58				2003–2010 (8 years)	Numerical Model (HYCOM, 1/12.5°)

Table 3. *Cont.*

Source	Volume Transports (Sv = 10^6 m^3/s)				Period of Data	Method
	Karimata Strait (1)	Bangka Strait (2)	Sunda Strait (3)	Eastern Boundary of the Java Sea (4)		
[30]	−0.87		−0.12	0.70	1950–2011 (62 years)	Numerical Model (HYCOM, 1/4°)
[8]	−0.50				November 2008–October 2009	ADCP measurement
[55]			0.24 (the boreal winter)/−0.83 (the boreal summer)		2008–2009	ADCP measurement
Present Study (2017)	−1.97	−0.12	−0.70	1.39	1950–2013 (64 years)	Numerical Model (HYCOM, 1/8°)

Note: (+)/(−) value indicates northward/southward transport in the Karimata and Bangka Straits. (+)/(−) value indicates eastward/westward transport in the Sunda Strait and Eastern Boundary of Java Sea.

Table 4. As in Table 3, but for the advective heat flux. Positive (negative) values indicate north or east (south or west) transport.

Source	Advective Heat Flux (PW = 10^{15} W)				Period of Data	Method	Notes
	Karimata Strait (1)	Bangka Strait (2)	Sunda Strait (3)	Eastern Boundary of the Java Sea (4)			
[4]	−0.113				1982–2003 (22 years)	Numerical Model (1/6°)	Annual mean value
[19]	−0.360				December 2007–November 2008 (1 year)	Roughly estimate from ADCP measurement	In the boreal winter month
[8]	−0.05				November 2008–October 2009	ADCP measurement	Annual mean value
Present Study (2017)	−0.204	−0.012	−0.072	0.148	1950–2013 (64 years)	Numerical Model (HYCOM, 1/8°)	Annual mean value

Note: (+)/(−) value indicates northward/southward transport in the Karimata and Bangka Straits. (+)/(−) value indicates eastward/westward transport in the Sunda Strait and Eastern Boundary of Java Sea.

3.2. Seasonal Variations of Volume Transport and Advective Heat Flux

Figure 3 displays the monthly means of advective heat flux and volume transport for 64 years (1950–2013). It represents the seasonal variations captured in each transect. Similarly, movement to the north or east is referred to as positive transport, whereas movement to the south or west is referred to as negative transport. Volume and advective heat flux both follow the same pattern, as seen in Figure 3. The mean of volume transport and advective heat flux in the Karimata Strait is always southward, with minima in June and maxima in January. The strongest southward transport occurs in January during the west monsoon and is associated with the southward wind in the Karimata Strait, allowing southward transport to strengthen. Similarly to the Karimata Strait, volume transport and advective heat flux in the Bangka Strait flow southward during the west monsoon in January and are captured the strongest among other months (Figure 3). The seasonal transports in the Sunda Strait and EBoJS are elaborated on in the Discussion section.

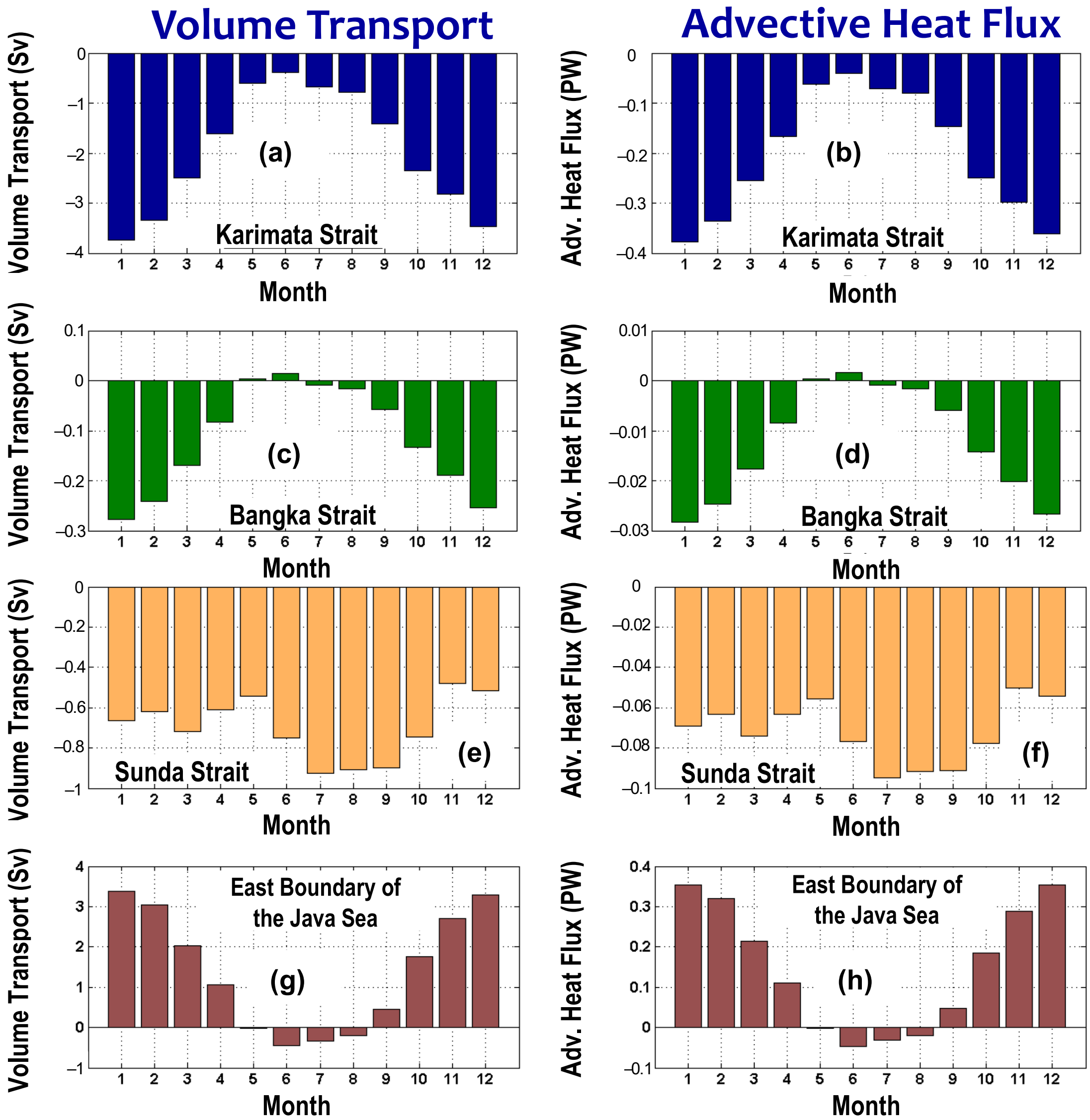

Figure 3. Monthly means of volume transport (**a**,**c**,**e**,**g**) and advective heat flux (**b**,**d**,**f**,**h**) in the Karimata Strait (**a**,**b**), Bangka Strait (**c**,**d**), Sunda Strait (**e**,**f**), and East Boundary of Java Sea (EBoJS) (**g**,**h**). Positive transport in the Karimata and Bangka Straits (Sunda and East Boundary of the Java Sea) denotes a northward (eastward), negative transport in the Karimata and Bangka Straits (Sunda and East Boundary of the Java Sea) denotes a southward (westward).

3.3. Time-Frequency Distributions (Power Spectral Density) of the Volume Transport

Figure 4 depicts the energy spectrum data for all ocean current transects over a 64-year period. The ocean current's energy spectrum is an example of how the volume transport might vary. These findings demonstrate that the patterns for the main signals in the Karimata Strait, Bangka Strait, and EBoJS are comparable. The 12-month periods has the most energy of the three transects, indicating that the monsoon has a substantial influence. In contrast, the Sunda Strait has relatively strong energy from intra-seasonal and 12-month periods. As a result of various phenomena, including the Kelvin waves and MJO, the Sunda Strait experienced a strong intra-seasonal period.

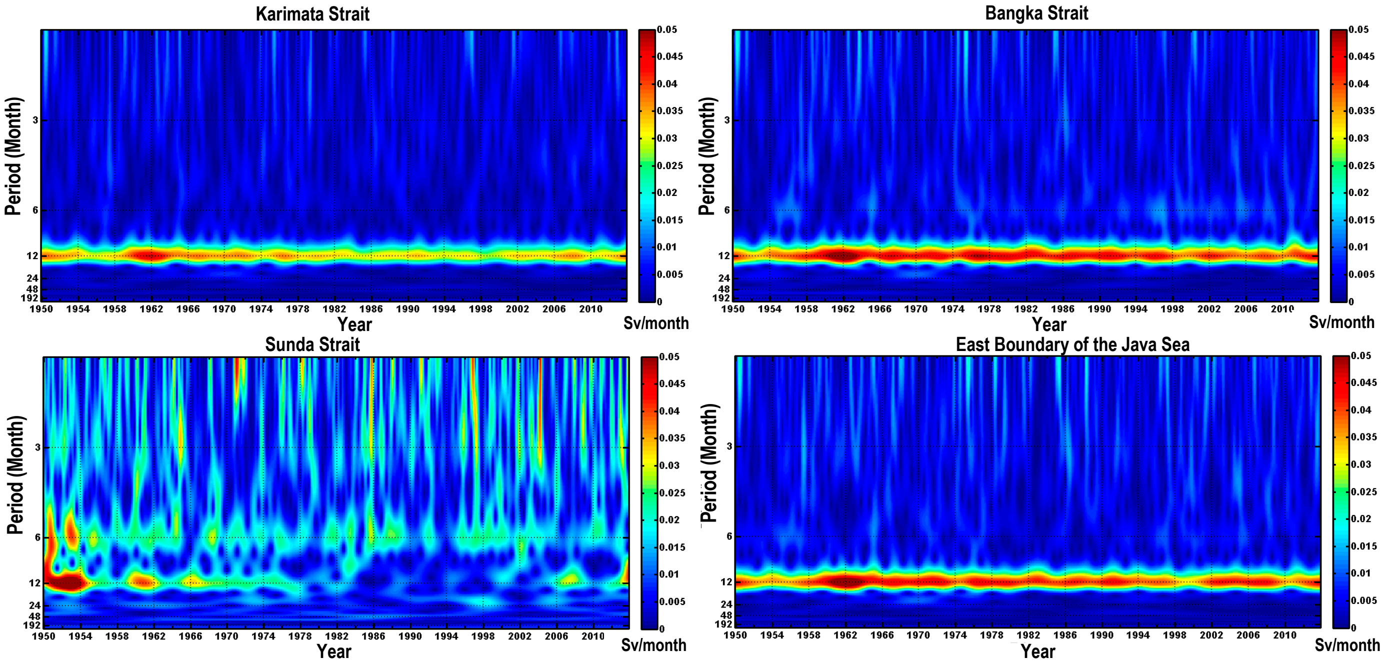

Figure 4. Ocean current energy distribution along each transect (1950–2013).

3.4. Energy Spectra of the Volume Transport

As a periodogram, Figure 5a,d display the ocean current energy spectrum and volume transport in the Karimata Strait and Sunda Strait, respectively. The periodogram reveals that the main period for both volume transport and ocean currents in this strait is identical. The one-year cycle of the monsoon winds, which has an impact on the 12-month periods, is predominant. Other prominent periods of the energy scale are enlarged in Figure 5b,c,e,f. The results show that there is also inter-annual variability with periods of 18 months (1.5 years), 23 months (2 years), 37 months (3 years), 45 months (3.75 years), 51 months (4.25 years), and 77 months (6.4 years), as well as intra-seasonal variability with periods of 3 months, 6 months, and 9 months. In addition to inter-annual, semi-annual, and intra-seasonal variability, the inter-decadal scale variability was found to have relatively significant energy over 256 months (21.3 years) and 384 months (32 years). Additionally, the energies are highly likely to be influenced by the 13- and 14-month signals.

3.5. Monthly and Interannual Variability of the Volume Transport (1950–2013)

According to the signal analysis results, the inter-annual variability in the four transects was indicated by a period ranging from 1.5–6.5 years. The time series graphic in Figure 6 illustrates the inter-annual variability of transport, which frequently strengthens and weakens over a 1.5–6-year period. The impact of ONI and DMI on transport strength is examined to conduct an inter-annual variability study. It is found that the Java Sea, interoceanic passage seasonal transports play a dual role in the total ITF from the Pacific to the Indian Oceans.

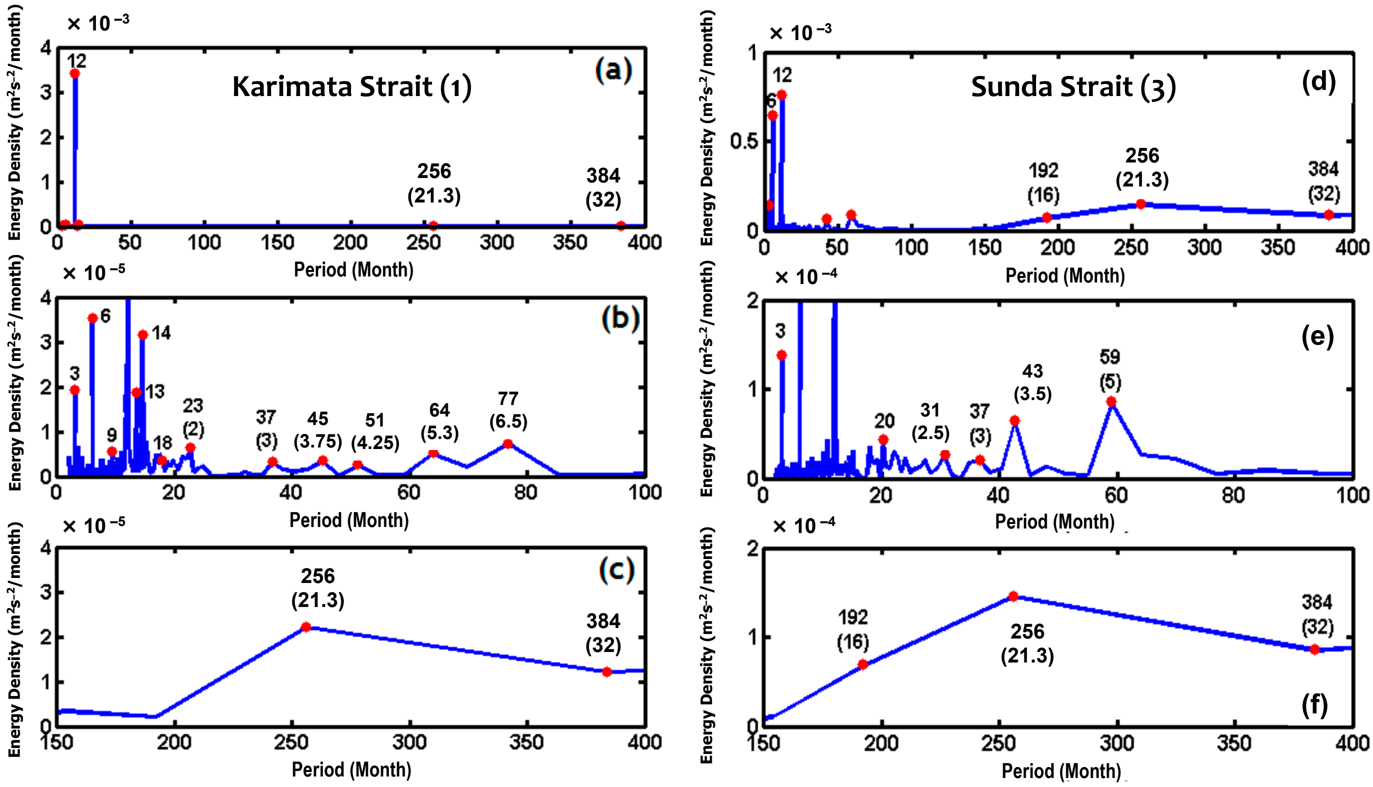

Figure 5. Periodogram of current energy spectra (**a**) and magnification (**b**,**c**) in the Karimata Strait and identical to (**d**–**f**) but in the Sunda Strait. Numbers in the horizontal axis are periods in months (year).

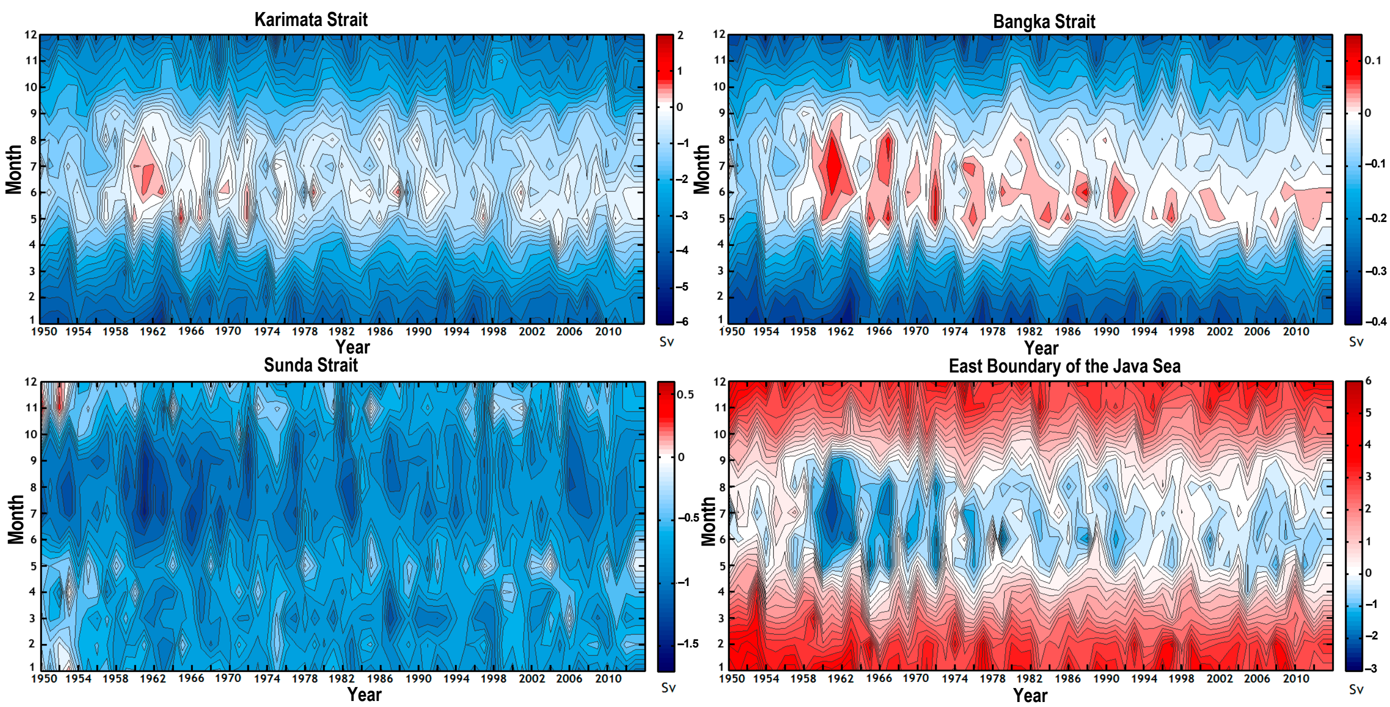

Figure 6. Time-series contours for volume transport, 1950–2013 (in Sv). Year is displayed on the x-axis, while month is displayed on the y-axis. While the red color (positive transport) in the Karimata and Bangka Straits (Sunda Strait and East Boundary of the Java Sea) denotes a northward (eastward), the blue color (negative transport) in the Karimata and Bangka Straits (Sunda Strait and East Boundary of the Java Sea) denotes a southward (westward).

Volume transport in the Karimata and Bangka Straits follows a similar pattern, but since the inter-annual effects in the Bangka Strait are more visible, this discussion is concentrated on the Bangka and Sunda Straits. From 1950 to 1982, the volume of transport in the Bangka Strait is depicted in Figure 7. Figure 7b,c show the ONI and DMI time series for the same year, allowing us to see the impact of ENSO and Dipole Mode (DM) events on volume transport.

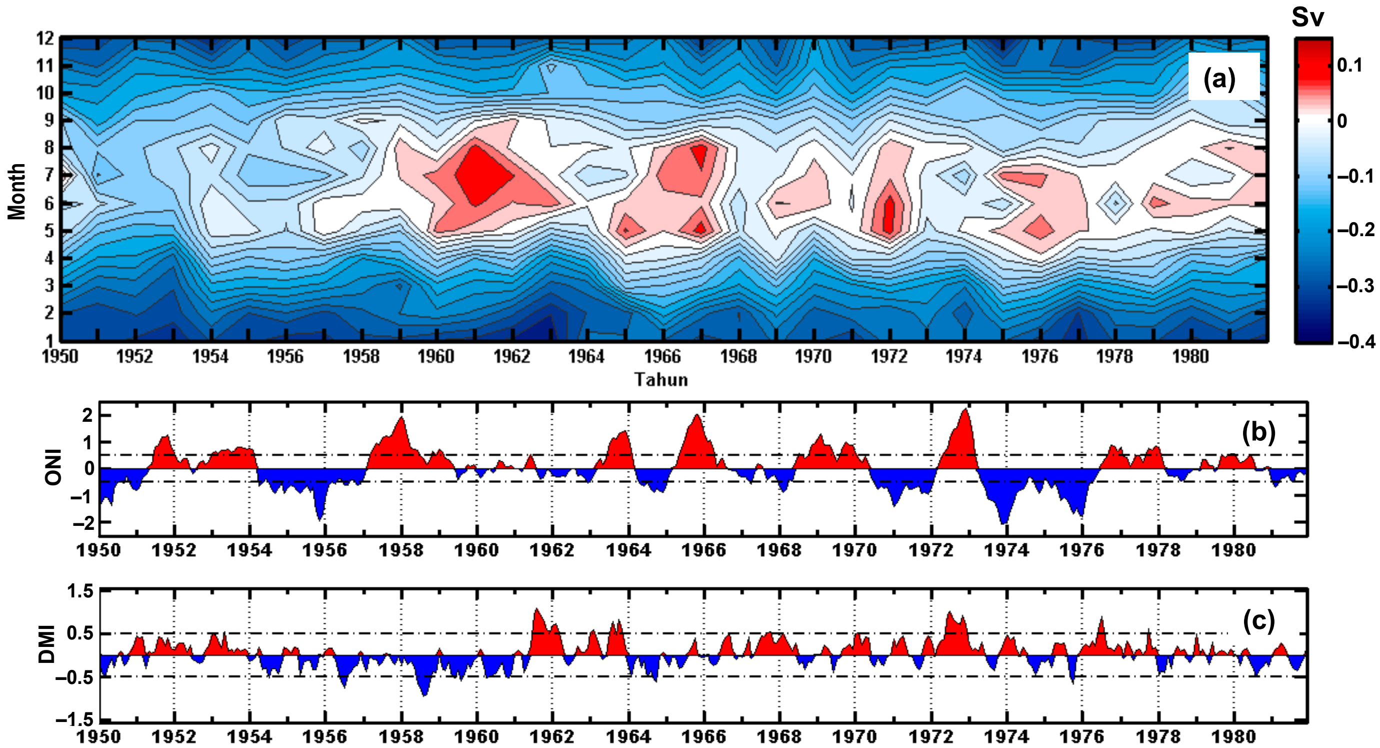

Figure 7. Volume transport time series in the Bangka Strait from 1950 to 1982 in a contour diagram (**a**). Time series of ONI (**b**) and DMI (**c**). While the red color (positive transport) denotes north transport, the blue color (negative transport) denotes south transport.

Inter-annual forcing associated with ENSO and IOD influenced volume transport in the Sunda Strait, as in the Bangka Strait and other Java Sea interoceanic passages (Figure 8).

3.6. Long-Term Trend of the Volume Transport and Advective Heat Flux in the Karimata Strait, Sunda Strait, and Eastern Boundary of Java Sea (EBoJS)

3.6.1. Karimata Strait

The time-series graph of advective heat flux and volume transport in the Karimata Strait is shown in Figure 9. The graph depicts a linear trend, but because the slope is so gentle, it is difficult to discern the trend. Therefore, it is enlarged to see the slope of the trend more clearly (Figure 9c,d). Volume transport is increasing in the Karimata Strait. In this transect, the meridional wind speed is positive and follows a positive trend (Figure 9e).

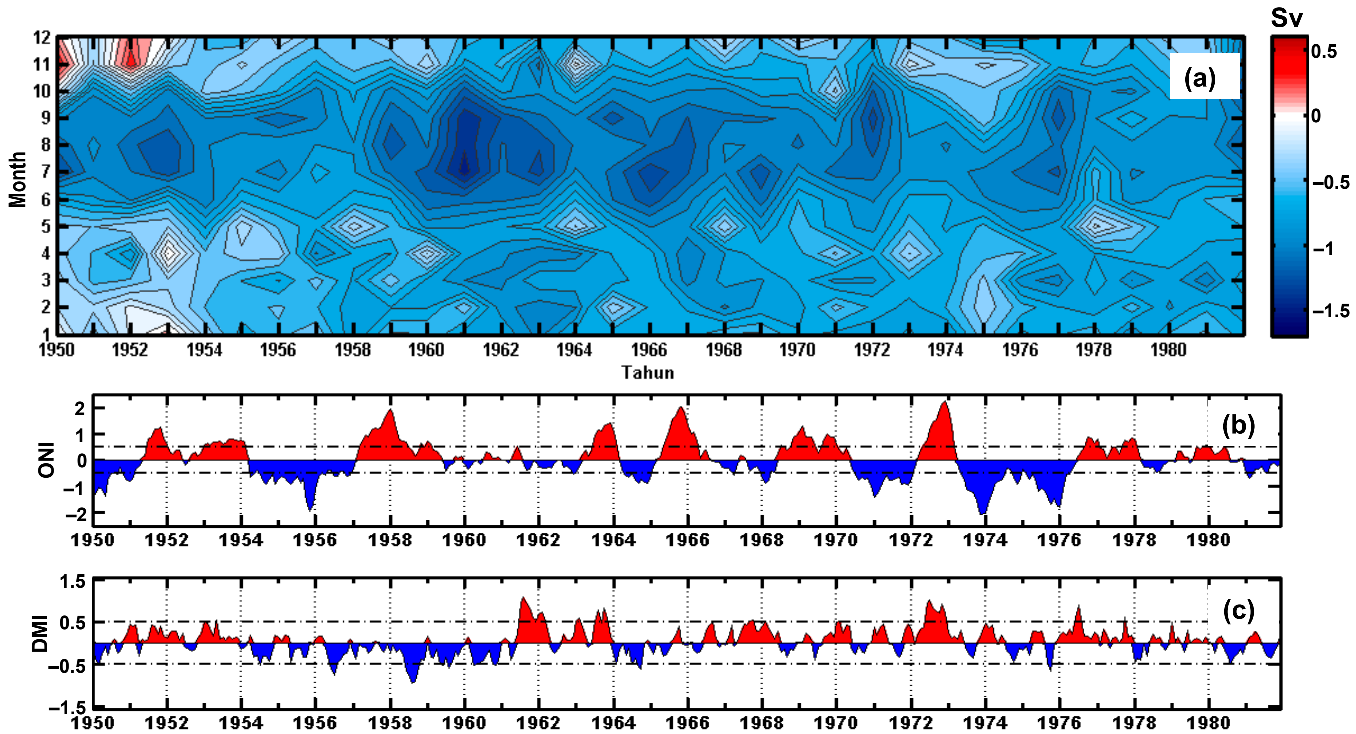

Figure 8. As in Figure 7, but for Sunda Strait. Volume transport in a contour diagram (**a**), time series of ONI (**b**) and DMI (**c**). While the red color (positive transport) denotes east transport, the blue color (negative transport) denotes west transport.

3.6.2. Sunda Strait and Eastern Boundary of Java Sea (EBoJS)

The linear trends for volume transport and advective heat flux in the Sunda Strait and EBoJS are both in line with the linear trend of zonal wind speed in the transects. The volume transport and advective heat flux in the Sunda Strait are both negative (Figure 10), indicating that the transport is moving west. However, in East Java, where the mean transport is positive (Figure 11), the transport moves eastward even though both linear trends are negative. A schematic of volume transport patterns and advective heat flux in the Java Sea is shown in Figure 12. The inflow-outflow in the Java Sea interoceanic passage is depicted in Table 5.

Table 5. Summary of Java Sea interocean passage inflow-outflow distribution during 1950–2013.

The Java Sea Interoceanic Passages	Direction of Transports	In the Period 1950–2013 (64 Years)	
		Total Increase (+ Value)/Decrease (− Value)	
		Volume Transport (Sv)	Advective Heat Flux (PW)
Eastern Boundary of Java Sea	Outflow	−0.07680	−0.00384
Karimata and Bangka Strait	Inflow	−0.06144	−0.00385
Sunda Strait	Outflow	0.01536	0.00384

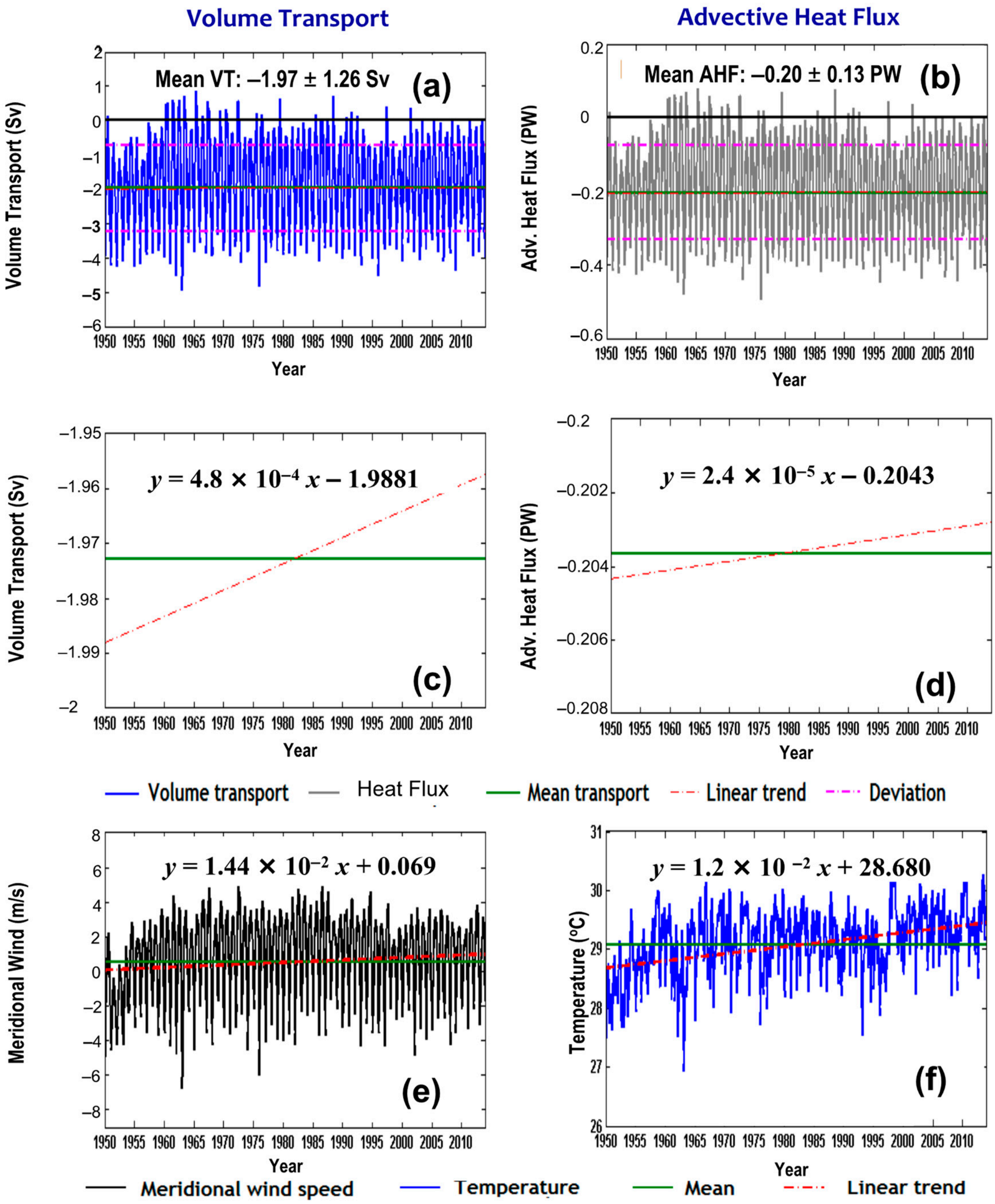

Figure 9. Time series graph of volume transport (**a**) and advective heat flux (**b**) during 1950–2013 in the Karimata Strait. Linear trend of volume transport (**c**) and advective heat flux (**d**). Time series graph of meridional wind speed (**e**) and temperature (**f**) in the Karimata Strait.

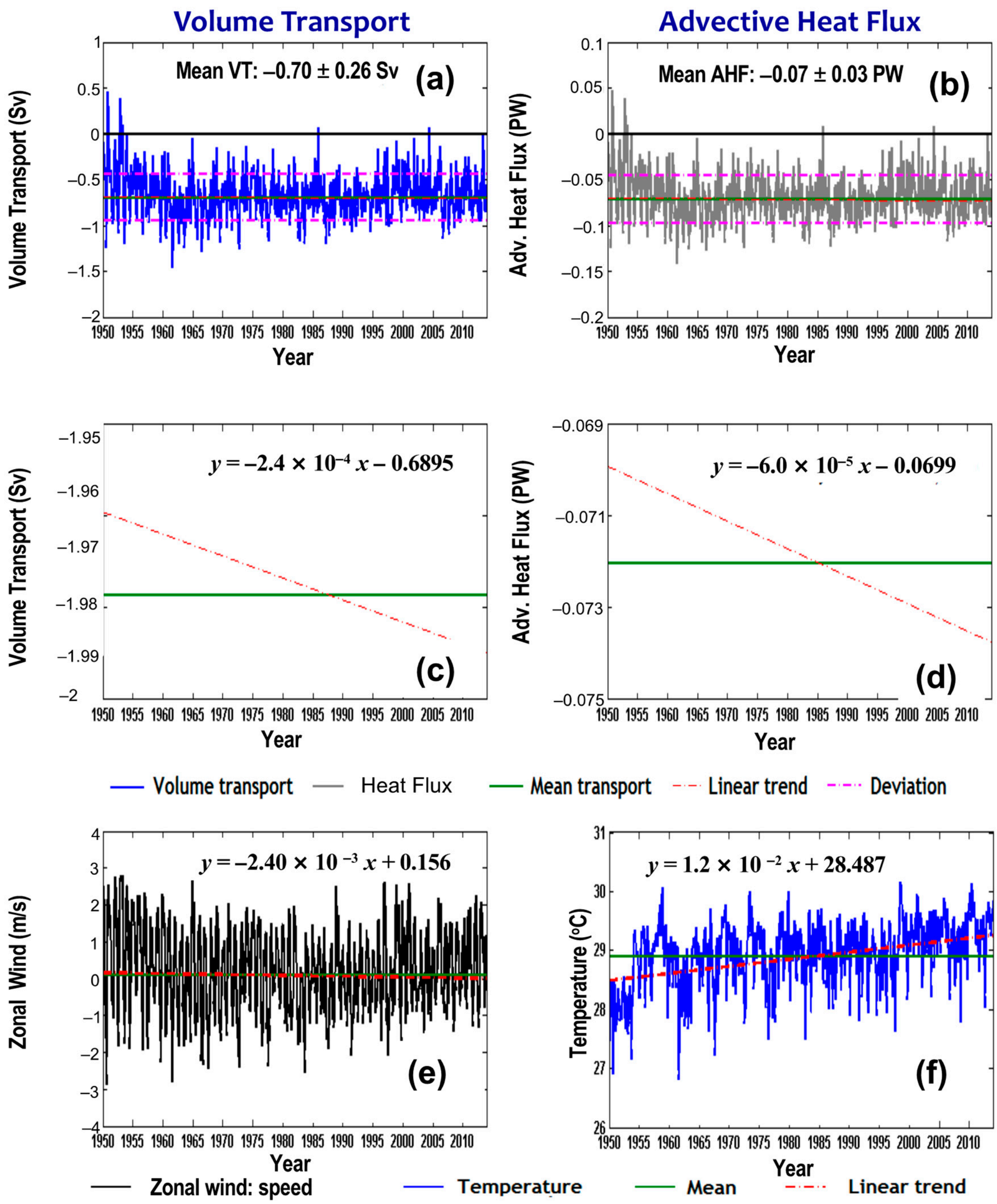

Figure 10. As in Figure 9 but for Sunda Strait. Time series graph of volume transport (**a**) and advective heat flux (**b**) during 1950–2013. Linear trend of volume transport (**c**) and advective heat flux (**d**). Time series graph of zonal wind speed (**e**) and temperature (**f**).

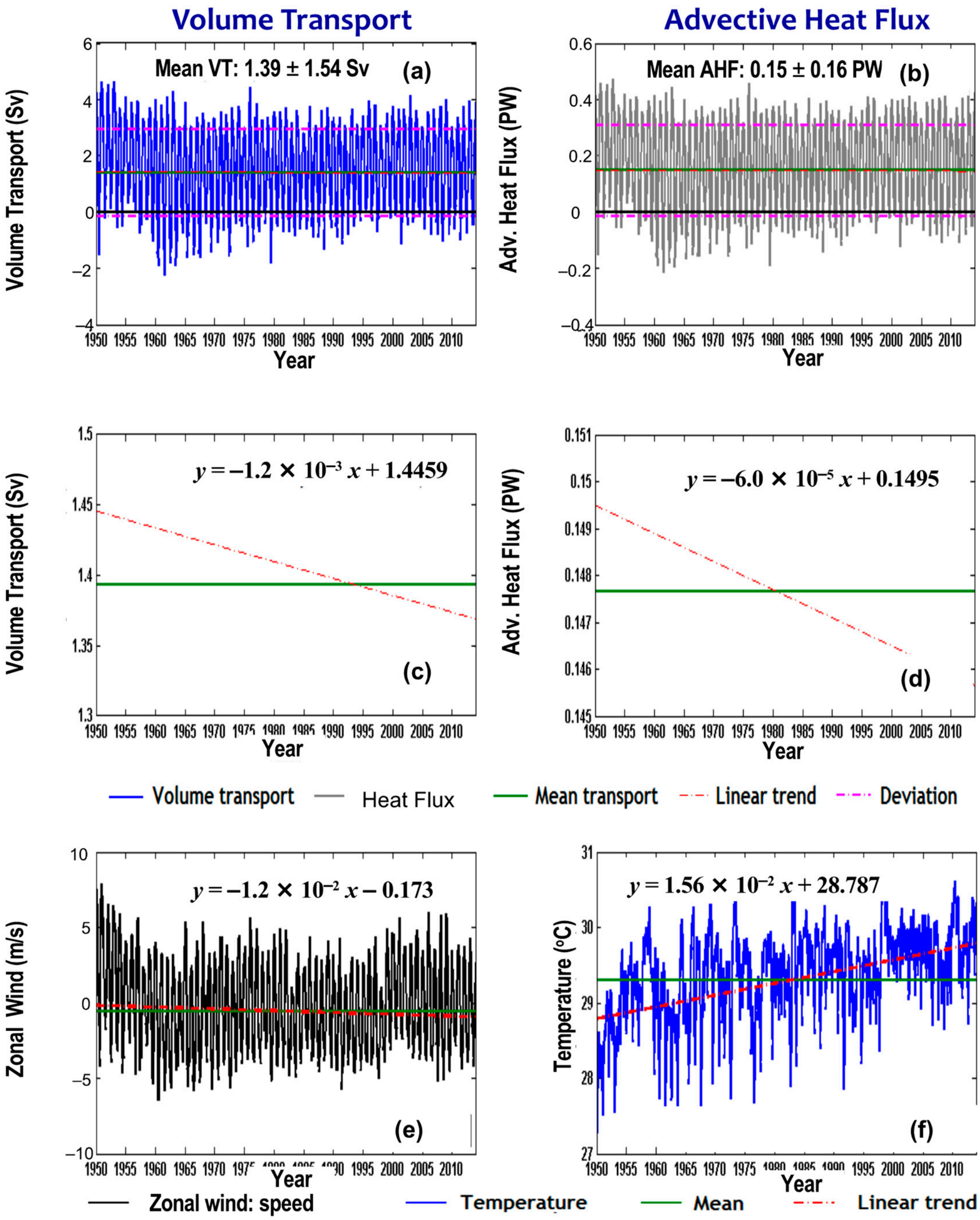

Figure 11. As in Figure 9 but for Eastern Boundary of Java Sea. Time series graph of volume transport (**a**) and advective heat flux (**b**) during 1950–2013. Linear trend of volume transport (**c**) and advective heat flux (**d**). Time series graph of zonal wind speed (**e**) and temperature (**f**).

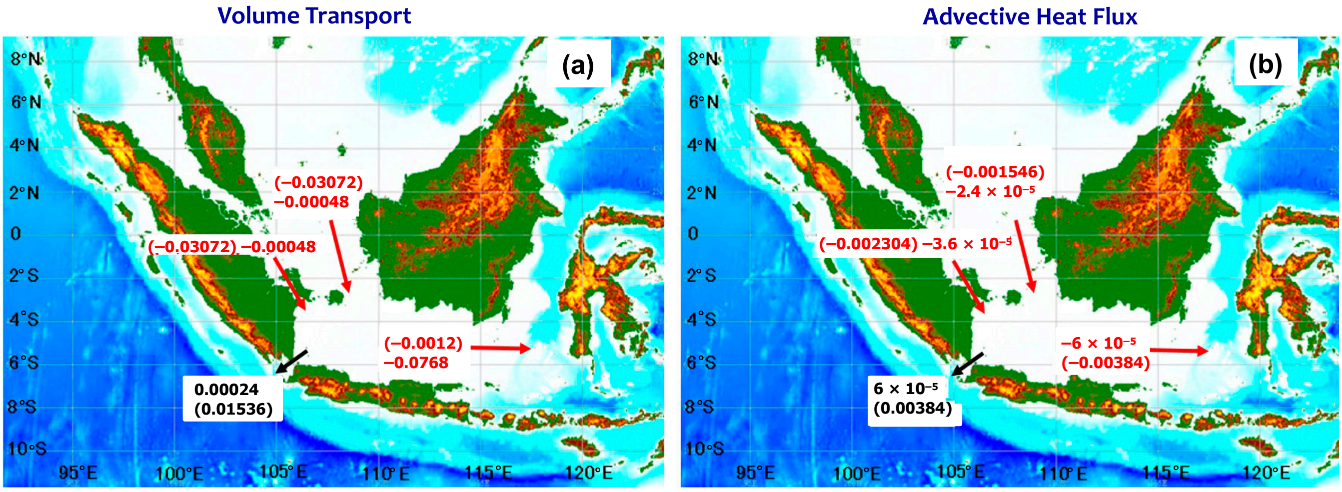

Figure 12. Trends in volume transport (**a**) (in Sv/year) and advective heat flux (**b**) (in PW/year) in the Java Sea. Arrows indicate the direction of mean transport. The black color and positive (red and negative) values indicate the strengthening (weakening) of the transport. Values without brackets: (+) the increased trend of the volume transport (Sv/yr) or advective heat flux (PW/yr), (−) the decreased trend of the volume transport (Sv/yr) or advective heat flux (PW/yr). Values in brackets: (+) total increase of the volume transport (Sv) or advective heat flux (PW) for 64 years (1950–2013), (−) total decrease of the volume transport (Sv) or advective heat flux (PW) for 64 years (1950–2013).

3.7. Interoceanic Volume Transport, Advective Heat Flux, and Heat Budgets

The typical volume of movement into and out of the Java Sea is depicted in Figure 13a and Table 6. A volume transport of 2.09 Sv enters the Karimata and Bangka Straits, and a volume transport of 2.09 Sv exits those straits. When the inflow and outflow values of the Java Sea are equal, the sea is in equilibrium. Because there is no excessive influx or outflow, the water level in these bodies of water remains constant. Figure 13b and Table 7 both show how heat moves into and out of the Java Sea. A total of 0.216 PW of advective heat flux enters the Karimata and Bangka Straits and exits via the Sunda Strait and East Java with a greater flow (0.220 PW).

Table 6. A mean volume transport in the Java Sea. Positive (negative) values indicate inflow (outflow) transport.

The Java Sea Interoceanic Passages	Mean Volume Transport (Sv)	Percentage (%)	Description
Karimata Strait	1.97	94.26	inflow
Bangka Strait	0.12	5.74	inflow
Sunda Strait	−0.70	33.50	outflow
East Boundary of Java Strait	−1.39	66.50	outflow
Inflow–Outflow	0.00	0.00	outflow = inflow

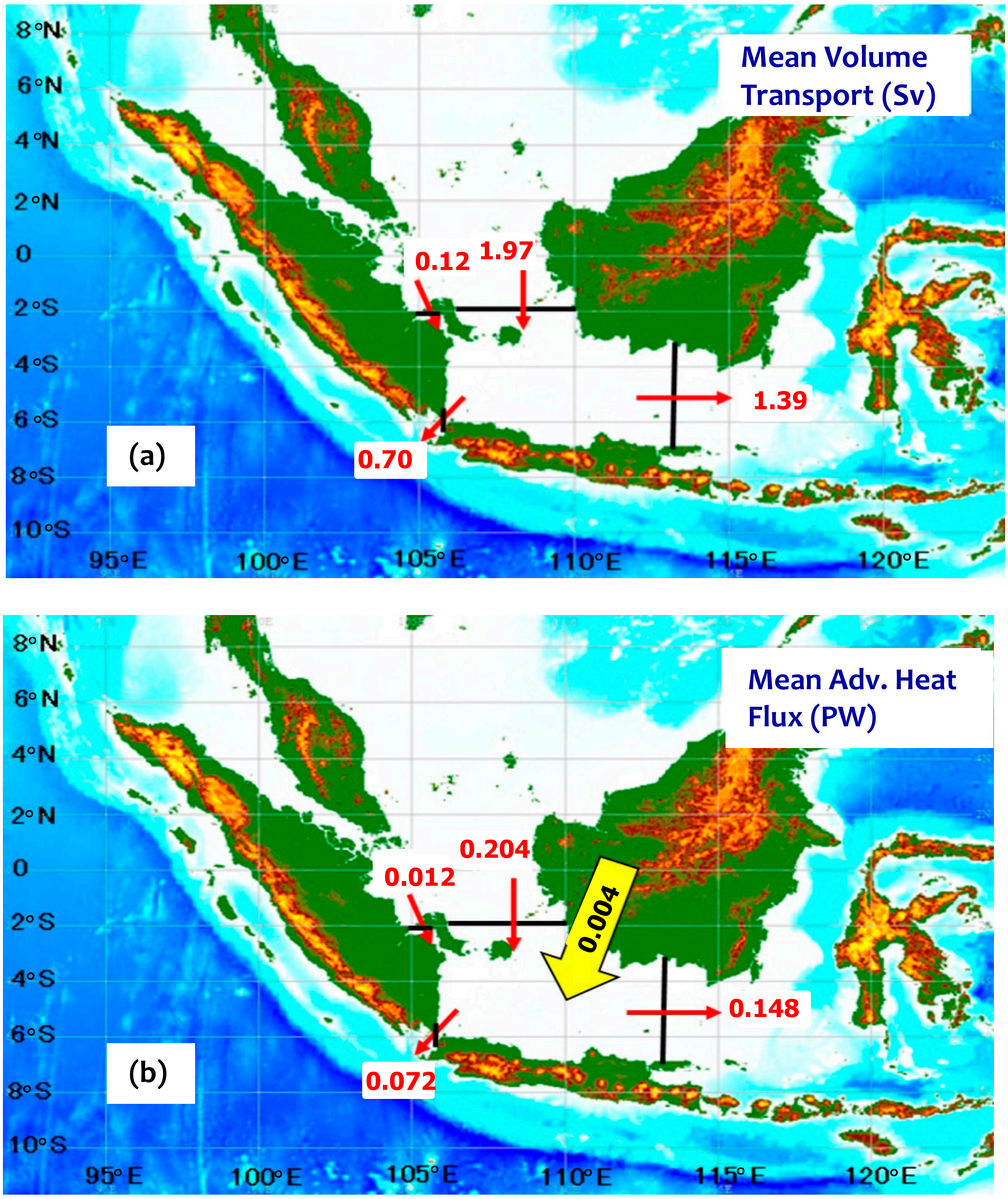

Figure 13. Scheme of inflow–outflow of volume transport (**a**) and advective heat flux (**b**) in the Java Sea. The yellow arrows indicate heat input from the atmosphere (in PW).

Table 7. Mean advective heat flux in the Java Sea. Positive (negative) values indicate inflow (outflow) transport.

The Java Sea Interoceanic Passages	Mean Advective Heat Flux (PW)	Percentage (%)	Description
Karimata Strait	0.204	92.73	inflow
Bangka Strait	0.012	5.45	inflow
Sunda Strait	−0.072	32.73	outflow
East Boundary of Java Sea	−0.148	67.27	outflow
Inflow-Outflow	−0.004	1.82	outflow > inflow

4. Discussion

According to the zonal and meridional volume transport and advective heat flux through the boundaries of the Java Sea's calculation performed for this study, the mean of volume transport in the Bangka Strait moves south (similar to the Karimata Strait) with a value of −0.12 Sv (Table 3). The volume transport through the Karimata Strait is noticeably greater than through the Bangka Strait due to its smaller size (Table 3). Both, however, increase the amount of inflow transport to the Java Sea. Moreover, since volume is always carried westward over the Sunda Strait, the mean of volume transport will always be negative, as shown in Table 3. The amount of transport that passes through the Sunda Strait on its way west indicates that it serves as a volumetric exit route from the Java Sea. In addition to the Sunda Strait, the canals of East Java act as conduits for volume transport exits from the Java Sea. Meanwhile, the mean volume transport in the Eastern boundary of the Java Sea (EBoJS) exits from the Java Sea and toward the east, according to a positive transport (Table 3). Similar to volume transport, advective heat flux reveals a southward flow through the Karimata Strait, Bangka Strait, westward flow from Java Sea into Sunda Strait, and an eastward flow through the EBoJS (Table 4).

In the seasonal variation, the wind in the Bangka Strait moves north during the east monsoon, resulting in northward transport. This is due to the Bangka Strait's shallow depth (30 m), which allows the wind's forcing to spread from the surface to the bottom of the strait. Meanwhile, the Karimata Strait is deeper (by approximately 50 m) compared to the Bangka Strait; hence wind forcing only affects the surface; similarly, the east monsoon weakens southward flow but does not change the direction of transport. Moreover, due to the vast cross-sectional area of the Karimata Strait, the wind's force cannot outweigh the substantial amount of transport flowing south. In the Sunda Strait, the westward volume transport and advective heat flux that occur year-round are highly exceptional associated with the difference in water levels between the Java Sea and the Indian Ocean. Despite this, monsoons continue to contribute to the strength of transport. According to Figure 3e,f, the east monsoon in July is the strongest, while the westward transport is the weakest in November. Furthermore, the Sunda Strait exhibits intra-seasonal variation, as evidenced by the strong flow in March and August and the weak transport in May and November. The Sunda Strait's location, which is traversed by intra-seasonal phenomena like Kelvin waves and MJO that can impede outflow from the Sunda Strait, explains the intra-seasonal variability that occurs there. Kelvin waves caused by a Wyrtki Jet in the equatorial Indian Ocean that propagate along the west coast of Sumatra and the south coast of Java depict intra-seasonal fluctuation with a duration of 35–90 days, according to [56,57]. While in the EBoJS, the dominant transport flows eastward and reaches its maximum in January to coincide with the west monsoon, while eastward transport weakens and even reverses westward and reaches its maximum value in June to coincide with the east monsoon. To summarize, the Java Sea interoceanic passage seasonal transports play a double role in the total ITF from the Pacific to the Indian Oceans. First, during the boreal winter (summer), the Karimata Strait, Bangka Strait, and the EBoJS transports reduce (enhance) the main ITF in the Makassar Strait. Second, in general, by exporting water from the Java Sea into the Indian Ocean, the Sunda Strait transport contributes to the ITF transport for each season, whereas during the boreal summer, the Sunda Strait transport contributes the most to the ITF.

To characterize dominant signals that influence volume transport for further analysis, a power spectral density (PSD) measurement was performed. The annual monsoon signals dominate volume transports through the Karimata Strait, the Bangka Strait, and the EBoJS. Volume transport through the Sunda Strait, however, is dominated not only by an annual signal monsoon but also by intra-seasonal and semi-annual signals. As suggested by [55], the intra-seasonal and semi-annual signals at the Sunda Strait may be associated with the intrusion of coastal Kelvin waves. However, more research is needed to confirm the possibility of the Kelvin waves entering the Sunda Strait.

Moreover, energy spectrum analysis exhibits 13- and 14-month intervals. This is due to the monsoon season, which may begin earlier and end later than usual, shortening the period to less than 12 months [58]. Finally, it is briefly stated that inter-annual and decadal signals in the volume transports of the Karimata Strait and Sunda Strait exist, with both signals being stronger in the Sunda Strait than in the Karimata Strait. An annual monsoon signal dominates the volume transport through the Karimata Strait. Volume transport through the Sunda Strait, however, is dominated not only by an annual and semi-annual signal monsoon but also by intra-seasonal and inter-annual signals.

Furthermore, the monthly and inter-annual variability of volume transport is investigated from 1950 to 2013 in Bangka Strait and Sunda Strait due to the visible inter-annual effects. It was found that from 1978 to 1979, ONI and DMI conditions were typical for each season. During the west monsoon, the transport typically moves 3.52 Sv southward. Southern transport decreased to −3.03 Sv in 1969 due to the El Niño, which coincided with the west monsoon. In contrast, when La Niña occurred in 1955 and 1956, southward transport increased to −3.85 Sv. This is in line with [14], where the southward flow decreases during El Niño and increases during La Niña. Despite the fact that the positive dipole mode conditions should have weakened southern transport, the transport in 1962 during the west monsoon, which coincided with the positive dipole mode event, was −3.87 Sv, slightly higher compared to La Niña years of 1955–1956. Thus, the positive dipole mode had no discernible influence during the west monsoon. Southward transport is quite weak and occasionally moves northward under typical ONI and DMI conditions during the east monsoon. When the climate was normal in 1978–1979, the transport value was −0.45 Sv. During El Niño in the east monsoon of 1965, the southward transport decreased to −0.21 Sv, whereas the southward transport increased to −0.85 Sv during the La Niña in 1974. During the east monsoon of 1961, positive dipole mode resulted in extremely strong northward transport of 0.52 Sv, while negative dipole mode resulted in powerful southward transport of −0.91 Sv. The effect of ONI and DMI on the transitional season is the same as it is on the west and east monsoons; the dipole mode's influence is simply less visible during this time. Thus, inter-annual forcing from ENSO and IOD influenced volume transport in the interoceanic passages of the Bangka Strait and the Java Sea.

As mentioned in the Results section, inter-annual forcing associated with ENSO and IOD influenced volume transport in the Sunda Strait, Bangka Strait, and Java Sea interoceanic passages. During the west monsoon, transport in the Sunda Strait normally flows westward by −0.67 Sv, but during the positive dipole mode occurrences in 1962 and 1963, it strengthened to −0.69 Sv. During the El Niño and La Niña phenomena in 1966 and 1955, and 1956, respectively, it flowed westward by −0.61 Sv and −0.58 Sv. Due to its coincident timing with the west monsoon, the La Niña situation reveals a drop in transport capability, making the influence of La Niña, which should strengthen the transport to the west, impossible to see. It is clear that the east monsoon is an indicator of La Niña's influence. The positive dipole mode (1961) resulted in a very strong westward transport of −1.30 Sv, whereas the negative dipole mode (1958) resulted in a westward transport of −0.75 Sv during the east monsoon, compared to typical conditions (1978 and 1979) of −0.76 Sv. During the east monsoon, the Sunda Strait experiences the ENSO effect, though it is not as strong as the dipole mode. Westward transport decreased to −0.75 Sv during El Niño in 1957 but increased to −0.86 Sv during La Niña in 1976. During the transitional season, ONI and DMI have the same effect as the west and east monsoons. A study by [31] provided a similar justification for the positive and negative dipole modes of the Sunda Strait's corresponding strengthening and weakening of westward transport.

Along with the monthly and inter-annual variability, the long-term trend of volume transport and advective heat flux in the Karimata Strait, the Sunda Strait, and the EBoJS is investigated. The volume transport trend is increasing in the Karimata Strait, following the wind movement to the north (Figure 9e). This results in a southward volume transport in the Karimata Strait associated with the increasing speed of the northward wind. Advective heat flux, like volume transport, has a positive trend in the Karimata Strait, which means that advective heat flux moving southward is becoming weaker each year. More heat is being carried by advection due to the direction of the current and the rising temperature in the Karimata Strait. Likewise, the linear trends for volume transport and advective heat flux in the Sunda Strait and EBoJS are both in line with the linear trend of zonal wind speed in the transects. Since the westward wind-driven current is increasing, the volume transport and advective heat flux in the Sunda Strait are both negative (Figure 10), indicating that the transport is moving to the west, following the wind-driven current. However, in EBoJS, the mean transport is positive (Figure 11), indicating the transport is moving eastward even though both linear trends are negative due to a stronger influence of a westward wind-driven current.

To analyze the in–out volume transport among the interoceanic bodies, advective heat flux and heat budgets are calculated. It was discovered that an equilibrium in–outflow of volume transport of up to 2.09 Sv enters and exits the Karimata and Bangka Straits. Figure 13b and Table 7 both show how heat moves into and out of the Java Sea. It is also evident that the amount of advective heat flux that enters the Karimata and Bangka Straits and exits via the Sunda Strait and EBoJS is not balanced because the outflow is greater (0.220 PW) compared to the inflow (0.216 PW). This has been suggested due to the atmosphere's contribution of 0.004 PW heat to these waters.

To conclude, the interoceanic passages' volume transport and advective heat flux changes in the Java Sea associated with inter-annual remote forcing are summarized in Table 8.

Table 8. Inter-annual remote forcing on the Java Sea Interoceanic Passages.

The Java Sea Interoceanic Passages	El Niño	La Niña	Dipole Mode +	Dipole Mode –
The Karimata Strait and Bangka Strait	Southward transport (ST) reduces	ST enhances	ST enhances	ST reduces
The Sunda Strait	Westward transport (WT) reduces	WT enhances	WT enhances	WT reduces
The Eastern Boundary of Java Sea	Eastward transport (ET) enhances	ET reduces	ET reduces	ET enhances

In addition, Figure 14 exhibits that over the past 64 years (1950–2013), the southward volume transport (advective heat flux) through the Karimata Strait and Bangka Strait and the eastward volume transport (advective heat flux) in the EBoJS has decreased by about 4.8×10^{-4} Sv/yr (2.4×10^{-5} PW/yr), 4.8×10^{-4} Sv/yr (3.6×10^{-5} PW/yr), and 1.2×10^{-3} Sv/yr (6×10^{-5} PW/yr), respectively. Meanwhile, the Sunda Strait's decreasing trends of volume transport (advective heat flux) of 2.4×10^{-4} Sv/yr (6×10^{-5} PW/yr) through the inflow passages were associated with an increasing trend in the passages' northward meridional wind speed. Additionally, the increasing trend of westward zonal wind speed through the outflow passages is associated with the decreasing trend of east transport through the EBoJS and the increasing trend of west transport through the Sunda Strait.

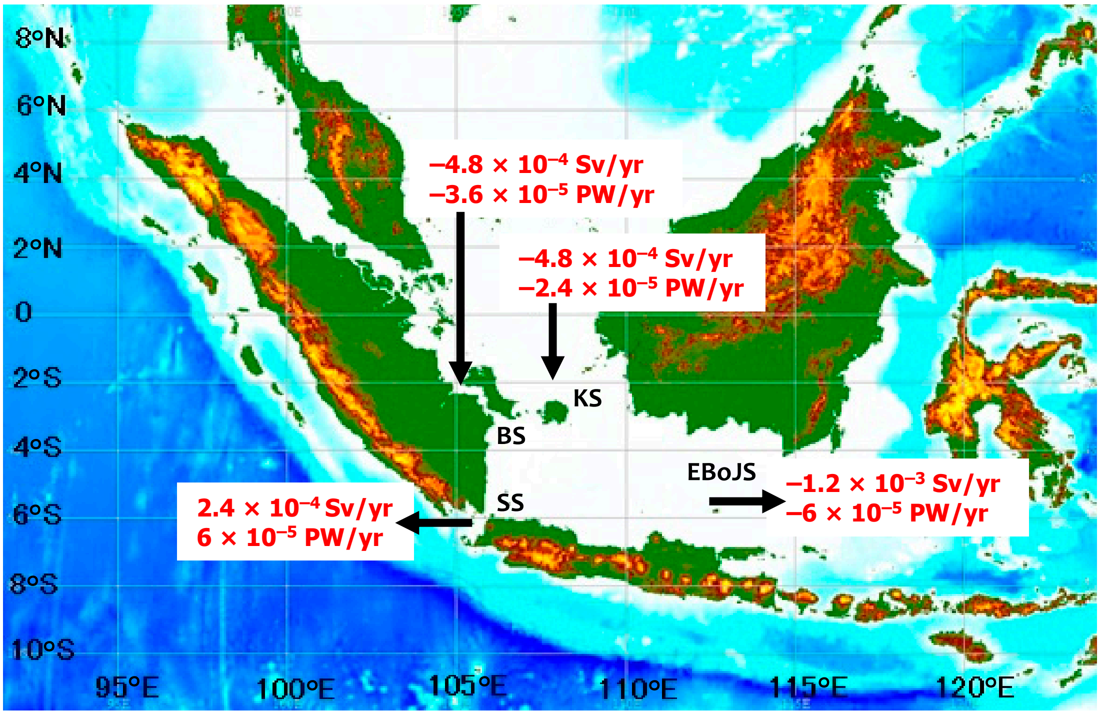

Figure 14. The southward volume transport and advective heat flux through the Karimata Strait (KS) and Bangka Strait (BS), the eastward transports in Eastern Boundary of the Java Sea (EBoJS), and the westward transports in Sunda Strait (SS), during 1950–2013.

5. Conclusions

Using a 1/8° global version of HYCOM, the long-term trend and variability of volume transport and advective heat flux through the Java Sea interoceanic passages were investigated from 1950 to 2013 (64 years). The water from the South China Sea enters the Java Sea via the Karimata and Bangka Straits, with annual mean volume transports of 1.97 Sv (94.26%) and 0.12 Sv (5.74%), respectively. Meanwhile, 1.39 Sv (66.5%) exits the Java Sea via its eastern boundary, and 0.7 Sv (33.5%) enters the Indian Ocean via the Sunda Strait. The heat in the South China Sea is transported to the Java Sea at a total rate of 0.216 PW via the inflow passages (the Karimata Strait and the Bangka Strait). In comparison, the total heat flux to the outflow passages (the Sunda Strait and the Eastern Boundary of the Java Sea) is 0.220 PW. This means that the total outward heat flux exceeds the total inward heat flux by 0.004 PW, implying that the Java Sea receives net heat gain from the air–sea exchange of its overlaying atmosphere. Inter-annual remote forcing associated with ENSO and IOD also influenced volume transport and advective heat flux through the Java Sea interoceanic passages. El Niño (La Niña) reduces (enhances) the southward transports in the Karimata and Bangka Strait. In contrast, the positive (negative) dipole mode enhances (reduces) the southward transports in the Karimata and Bangka Strait. Similar to Karimata and Bangka Strait, westward transport in Sunda Strait experienced a reduction (enhancement) during El Niño (La Niña) and during negative (positive) dipole mode. Meanwhile, in the EBoJS, the eastward transports reduce (enhance) during La Niña (El Niño) and during positive (negative) dipole mode. Furthermore, the southward transports decrease through the Karimata Strait and Bangka Strait, the eastward transports decrease in the EBoJS, and the westward transports decrease in the Sunda Strait during 1950–2013.

Author Contributions: Conceptualization, N.S.N.; methodology, F.H. and Y.N.; software, Y.N.; validation, F.H. and Y.N.; formal analysis, N.S.N., F.H. and R.R.; investigation, N.S.N., F.H. and R.R.; resources, Y.N.; data curation, Y.N.; writing—original draft preparation, R.R. and Y.N.; writing—review and editing, R.R. and N.S.N.; visualization, Y.N., N.S.N. and R.R.; supervision, N.S.N. and F.H.; project administration, N.S.N.; funding acquisition, N.S.N. All authors have read and agreed to the published version of the manuscript.

Funding: This study was funded by Institut Teknologi Bandung under PROGRAM RISET ITB year 2022, scheme RISET UNGGULAN ITB. Research Grand Contract No. 223/IT1.B07.1/TA.00/2022.

Data Availability Statement: Data sharing not applicable. No new data were created or analyzed in this study. Data sharing is not applicable to this article.

Conflicts of Interest: The authors declare no conflict of interest.

References

1. Feng, M.; Zhang, N.; Liu, Q.; Wijffels, S. The Indonesian throughflow, its variability and centennial change. *Geosci. Lett.* **2018**, *5*, 3. [CrossRef]
2. Vranes, K.; Gordon, A.L.; Ffield, A. The heat transport of the Indonesian Throughflow and implications for the Indian Ocean heat budget. *Deep. Sea Res. Part II Top. Stud. Oceanogr.* **2002**, *49*, 1391–1410. [CrossRef]
3. Yari, S.; Kovačević, V.; Cardin, V.; Gačić, M.; Bryden, H.L. Direct estimate of water, heat, and salt transport through the Strait of Otranto. *J. Geophys. Res. Ocean.* **2012**, *117*, C9. [CrossRef]
4. Fang, G.; Wang, Y.; Wei, Z.; Fang, Y.; Qiao, F.; Hu, X. Interocean Circulation and Heat and Freshwater Budgets of the South China Sea Based on a Numerical Model. *Dyn. Atmos. Ocean.* **2008**, *47*, 55–72. [CrossRef]
5. Zheng, Y.; Giese, B. Ocean heat transport in Simple Ocean Data Assimilation: Structure and mechanisms. *J. Geophys. Res.* **2009**, *114*, C11009. [CrossRef]
6. Sprintal, J.; Gordon, A.L.; Wijffels, S.E.; Feng, M.; Hu, S.; Koch-Larrouy, A.; Phillips, H.; Nugroho, D.; Napitu, A.; Pujiana, K.; et al. Detecting Change in the Indonesian Seas. *Front. Mar. Sci.* **2019**, *6*, 257. [CrossRef]
7. Kok, P.H.; Wijeratne, S.; Akhir, M.F.; Ali, F.S.M. Interconnection between the Southern South China Sea and the Java Sea through the Karimata Strait. *J. Mar. Sci. Eng.* **2021**, *9*, 1040. [CrossRef]
8. Susanto, R.D.; Zexun, W.; Rameyo, A.; Bin, F.; Shujiang, L.; Guohong, F. Observations of the Karimata Strait throughflow from December 2007 to November 2008. *Acta Oceanol. Sin.* **2013**, *32*, 1–6. [CrossRef]
9. He, Z.; Feng, M.; Wang, D.; Slawinski, D. Contribution of the Karimata Strait transport to the Indonesian Throughflow as seen from a data assimilation model. *Cont. Shelf Res.* **2014**, *92*, 16–22. [CrossRef]
10. Wei, Z.; Li, S.; Susanto, R.D.; Wang, Y.; Fan, B.; Xu, T.; Sulistiyo, B.; Adi, T.R.; Setiawan, A.; Kuswardani, A.; et al. An overview of 10-year observation of the South China Sea branch of the Pacific to Indian Ocean throughflow at the Karimata Strait. *Acta Oceanol. Sin.* **2019**, *38*, 1–11. [CrossRef]
11. Xu, T.F.; Wei, Z.X.; Susanto, R.D.; Li, S.J.; Wang, Y.G.; Wang, Y. Observed water exchange between the South China Sea and Java Sea through Karimata Strait. *J. Geophys. Res. Ocean.* **2021**, *126*, e2020JC016608. [CrossRef]
12. Gordon, A.L.; Susanto, R.D.; Vranes, K. Cool Indonesian throughflow is a consequence of restricted surface layer flow. *Nature* **2003**, *425*, 824–828. [CrossRef] [PubMed]
13. Fang, G.; Susanto, R.D.; Soesilo, I.; Zheng, Q.; Fangli, Q.; Zexun, W. A note on the South China Sea shallow interocean circulation. *Adv. Atmos. Sci.* **2005**, *22*, 946–954. [CrossRef]
14. Qu, T.; Du, Y.; Meyers, G.; Ishida, A.; Wang, D. Connecting the tropical Pacific with Indian Ocean through South China Sea. *Geophys. Res. Lett.* **2005**, *32*, L24609. [CrossRef]
15. Qu, T.; Meyers, G. *Seasonal Characteristics of Circulation in theSoutheastern Tropical Indian Ocean, Notes and Correspondence*; American Meteorological Society: Boston, MA, USA, 2005; pp. 255–267.
16. Wang, D.; Liu, Q.; Huang, R.X.; Du, Y.; Qu, T. Interannual variability of the South China Sea throughflow inferred from wind data and an ocean data assimilation product. *Geophys. Res. Lett.* **2006**, *33*, L14605. [CrossRef]
17. Tozuka, T.; Qu, T.; Yamagata, T. Dramatic impact of the South China Sea on the Indonesian throughflow. *Geophys. Res. Lett.* **2007**, *34*, L12612. [CrossRef]
18. Tozuka, T.; Qu, T.; Masumoto, Y.; Yamagata, T. Impacts of the South China Sea throughflow on seasonal and interannual variations of the Indonesian throughflow. *Dyn. Atmos. Oceans* **2009**, *47*, 73–85. [CrossRef]
19. Fang, G.; Susanto, R.D.; Wirasantosa, S.; Qiao, F.; Supangat, A.; Fan, B.; Wei, Z.; Sulistiyo, B.; Li, S. Volume, Heat, and Freshwater Transports from the South China Sea to Indonesian Seas in the boreal winter of 2007–2008. *J. Geophys. Res.* **2010**, *115*, C12020. [CrossRef]
20. Susanto, R.D.; Fang, G.; Soesilo, I.; Zheng, Q.; Qiao, F.; Wei, Z.; Sulistyo, B. New Surveys of a branch of the Indonesian Throughflow. EOS Trans. *AGU* **2010**, *91*, 261–263. [CrossRef]
21. Gordon, A.L.; Huber, B.A.; Metzger, E.J.; Susanto, R.D.; Hurlburt, H.E.; Adi, T.R. South China Sea Throughflow Impact on the Indonesian Throughflow. *Geophys. Res. Lett.* **2012**, *39*, LI1602. [CrossRef]

22. Suneet, D.; Kumar, M.A.; Atul, S. Upper ocean high resolution regional modeling of the Arabian Sea and Bay of Bengal. *Acta Oceanol. Sin.* **2019**, *38*, 32–50. [CrossRef]
23. Srivastava, A.; Suneet, D.; Mishra, A.K. Investigating the role of air-sea forcing on the variability of hydrography, circulation, and mixed layer depth in the Arabian Sea and Bay of Bengal. *Oceanologia* **2018**, *60*, 169–186. [CrossRef]
24. Han, L.; Zhang, S.; Xu, F.; Lu, J.; Lu, Z.; Ye, G.; Chen, S.; Xu, J.; Du, J. Simulations of sea fog case impacted by air–sea interaction over South China Sea. *Front. Mar. Sci.* **2022**, *9*, 1000051. [CrossRef]
25. Metzger, E.J.; Hurlburt, H.E. Coupled dynamics of the South China sea, the Sulu Sea, and the Pacific ocean. *J. Geophys. Res. Ocean.* **1996**, *101*, 12331–12352. [CrossRef]
26. Lebedev, K.V.; Yaremchuk, M.I. 2000. A diagnostic study of the Indonesian Throughflow. *J. Geophys. Res.* **2000**, *105*, 11243–11258. [CrossRef]
27. Fang, G.; Wei, Z.; Byung-Ho, C.; Kai, W.; Yue, F.; Wei, L. Interbasin freshwater, heat and salt transport through the boundaries of the East and South China Seas from a variable-grid global ocean circulation model. *Sci. China Ser. D Earth Sci.* **2003**, *46*, 149–161. [CrossRef]
28. Gong, D.; Wang, S. Definition of Antarctic Oscillation Index. *Geophys. Res. Lett.* **1999**, *26*, 459–462. [CrossRef]
29. Zhang, Y.; Rossow, W.B.; Stackhouse, P., Jr.; Romanou, A.; Wielicki, B.A. Decadal variations of global energy and ocean heat budget and meridional energy transports inferred from recent global data sets. *Clim. Dyn.* **2007**, *112*, D22101. [CrossRef]
30. Prianto, A. Variability of Mass Transport Across Indonesian and Surrounding Waters. Bachelor Thesis, Oceanography Study Program. Bandung Institute of Technology, Bandung, Indonesia, 2013.
31. Putri, M.R. Study of Ocean Climate Variability (1959–2002) in the Eastern Indian Ocean, Java Sea and Sunda Strait Using the HAMburg Shelf Ocean Model. Ph.D. Dissertation, Earth Science Department, University of Hamburg, Hamburg, Germany, 2005.
32. Du, Y.; Qu, T.; Xu, T.; Li, S.; Wei, Z. Three inflow pathways of the Indonesian Throughflow as seen from the simple ocean data assimilation. *Dyn. Atmos. Ocean.* **2010**, *50*, 233–256. [CrossRef]
33. Wang, Y. Seasonal variation of water transport through the Karimata Strait. *Acta Oceanol. Sin. Engl. Ed.* **2019**, *38*, 47–57. [CrossRef]
34. Keerthi, M.G.; Lengaigne, M.; Drushka, K.; Vialard, J.; Montegut, C.D.B.; Pous, S.; Levy, M.; Muraleedharan, P.M. Intraseasonal variability of mixed layer depth in the tropical Indian Ocean. *Clim. Dyn.* **2016**, *46*, 2633–2655. [CrossRef]
35. Keerthi, M.G.; Lengaigne, M.; Vialard, J.; Montégut, C.D.B.; Muraleedharan, P.M. Interannual variability of the Tropical Indian Ocean mixed layer depth. *Clim. Dyn.* **2013**, *40*, 743–759. [CrossRef]
36. Sofian, I. Simulation of The Java Sea Using an Oceanic General Circulation Model. *J. Ilm. Geomatika* **2007**, *13*, 1–14.
37. Sulistya, W.; Hartoko, A.; Prayitno, S.B. *The Characteristics and Variability of Sea Surface Temperature in Java Sea*; Meteorological and Geophysical Agency: Bali, Indonesia, 2007.
38. Nagara, A.N.; Sasongko, N.A.; dan Olakunle, O.J. *Introduction to Java Sea*; University of Stavanger: Stavanger, Norway, 2007.
39. Du, Y.; Qu, T.; Meyers, G. Interannual Variability of Sea Surface Temperature off Java and Sumatra in a Global GCM. *J. Clim.* **2008**, *11*, 2451–2465. [CrossRef]
40. Dieterich, C.; Wang, S.; Schimanke, S.; Groger, M.; Klein, B.; Hordoir, R.; Samuelsson, P.; Liu, Y.; Axell, L.; Hoglund, A.; et al. Surface Heat Budget over the North Sea in Climate Change Simulations. *Atmosphere* **2019**, *10*, 272. [CrossRef]
41. Wirasatriya, A.; Sugianto, D.N.; Helmi, M.; Maslukah, L.; Widiyandono, R.T.; Herawati, V.E.; Subardjo, P.; Handoyo, G.; Marwoto, J.; Suryoputro, A.A.D.; et al. Heat Flux Aspects on The Seasonal Variability of Sea Surface Temperature in The Java Sea. *Ecol. Environ. Conserv. Pap.* **2019**, *25*, 434–442.
42. IOC; IHO; dan BODC. *General Bathymetric Chart of the Ocean. Centenary Edition of the GEBCO Digital Atlas*; BODC: Liverpool, UK, 2003.
43. Smith, W.H.F.; Sandwell, D.T. Global Sea Floor Topography from Satellite Altimetry and Ship Depth Soundings. *Science* **1997**, *277*, 1956. [CrossRef]
44. Conkright, M.E.; Levitus, S.; Boyer, T.P. *World Ocean Atlas 1994 Volume 1: Nutrients*; NOAA: Washington, DC, USA, 1994.
45. Levitus, S.; Boyer, T.P. *World Ocean Atlas 1994 Volume 2: Oxygen*; NOAA: Washington, DC, USA, 1994.
46. Levitus, S.; Burgett, R.; Boyer, T.P. *World Ocean Atlas 1994 Volume 3: Nutrients*; NOAA: Washington, DC, USA, 1994.
47. Levitus, S.; Boyer, T.P. *World Ocean Atlas 1994 Volume 4: Temperature*; NOAA: Washington, DC, USA, 1994.
48. Kanamitsu, M.; Ebisuzaki, W.; Woolen, J.; Yang, S.-K.; Hnilo, J.J.; Fiorino, M.; Potter, G.L. NCEP–DOE AMIP-II Reanalysis (R-2). *Am. Meteorol. Soc. J.* **2002**, *83*, 1631–1644. [CrossRef]
49. Hanifah, F.; Ningsih, N.S.; Sofian, I. Dynamics of eddies in the southeastern tropical Indian Oceean. *J. Phys. Conf. Ser.* **2016**, *739*, 012042. [CrossRef]
50. Hanifah, F.; Ningsih, N.S. The characteristic of eddies in the Banda Sea. *Adv. Appl. Fluid Mech.* **2016**, *19*, 889. [CrossRef]
51. Ningsih, N.S.; Azhar, M.A.; Hanifah, F.; Kushadiwijayanto, A.A. *Eddy Variability Study to Identify Water Fertility as an Effort to Strengthen National Food Security (Case Study: Java's Southern Waters)*; ITB Batch II Research and Innovation Program Report; Bandung Institute of Technology: Bandung, Indonesia, 2014.
52. Ningsih, N.S.; Sakina, S.L.; Susanto, R.D.; Hanifah, F. Simulated zonal current characteristics in the southeastern tropical Indian Ocean (SETIO). *Ocean Sci.* **2021**, *17*, 1115–1140. [CrossRef]
53. Wannasingha, U.; Webb, D.J.; de Cuevas, B.A.; Coward, A.C. On the Indonesian Throughflow in the OCCAM Model. 2003. Available online: http://www.noc.soton.ac.uk/ (accessed on 7 April 2015).

54. Yaremchuk, M.; McCreary, J.; Yu, Z.; Furue, R. The South China Sea throughflow retrieved from climatological data. *J. Phys. Oceanogr.* **2009**, *39*, 753–767. [CrossRef]
55. Susanto, R.D.; Wei, Z.; Adi, T.R.; Zheng, Q.; Fang, G.; Fan, B.; Supangat, A.; Agustiadi, T.; Li, S.; Trenggono, M.; et al. Oceanography surrounding Krakatau Volcano in the Sunda Strait, Indonesia. *Oceanography* **2016**, *2*, 228–237.
56. Syamsudin, F.; Kaneko, A. Numerical and Observational Estimates of Indian Ocean Kelvin Wave Intrusion into Lombok Strait. Hiroshima University. *Geophys. Res. Lett.* **2004**, *31*, L24307. [CrossRef]
57. Iskandar, I.; Mardiansyah, W.; Matsumoto, Y.; Yamagata, T. Intraseasonal Kelvin Waves Along The Southern Coast of Sumatra and Java. *J. Geophys. Res.* **2005**, *110*, C04013. [CrossRef]
58. Goswami, B.N.; Xavier, P.K. ENSO control on the south Asian monsoon through the length of the rainy season. *Geophys. Res. Lett.* **2005**, *32*, L18717. [CrossRef]